Please cite this article in press as: Blumberg et al., Spatiotemporal Structure of REM Sleep Twitching Reveals Developmental Origins of Motor Synergies, Current Biology (2013), http://dx.doi.org/10.1016/j.cub.2013.08.055

Current Biology *23*, 1–10, November 4, 2013 ©2013 Elsevier Ltd All rights reserved http://dx.doi.org/10.1016/j.cub.2013.08.055

Article

Spatiotemporal Structure of REM Sleep Twitching Reveals Developmental Origins of Motor Synergies

Mark S. Blumberg,[1,2,3,*] Cassandra M. Coleman,[1] Ashlynn I. Gerth,[1] and Bob McMurray[1,3,4]

[1]Department of Psychology, The University of Iowa, Iowa City, IA 52242, USA

[2]Department of Biology, The University of Iowa, Iowa City, IA 52242, USA

[3]Delta Center, The University of Iowa, Iowa City, IA 52242, USA

[4]Department of Communication Sciences and Disorders, The University of Iowa, Iowa City, IA 52242, USA

Summary

Background: During active (or REM) sleep, infant mammals exhibit myoclonic twitches of skeletal muscles throughout the body, generating jerky, discrete movements of the distal limbs. Hundreds of thousands of limb twitches are produced daily, and sensory feedback from these movements is a substantial driver of infant brain activity, suggesting that they contribute to motor learning and sensorimotor integration. It is not known whether the production of twitches is random or spatiotemporally structured, or whether the patterning of twitching changes with age; such information is critical for understanding how twitches contribute to development.

Results: We used high-speed videography and 3D motion tracking to assess the spatiotemporal structure of twitching at forelimb joints in 2- and 8-day-old rats. At both ages, twitches exhibited highly structured spatiotemporal properties at multiple timescales, including synergistic and multijoint movements within and across forelimbs. Hierarchical cluster analysis and latent class analysis revealed developmental changes in twitching quantity and patterning. Critically, we found evidence for a selectionist process whereby movement patterns at the early age compete for retention and expression over development.

Conclusions: These findings indicate that twitches are not produced randomly but are highly structured at multiple timescales. This structure has important implications for understanding brain and spinal mechanisms that produce twitching, and the role that sensory feedback from twitching plays in sensorimotor system development. We propose that twitches represent a heretofore-overlooked form of motor exploration that helps animals probe the biomechanics of their limbs, build motor synergies, and lay a foundation for complex, automatic, and goal-directed wake movements.

Introduction

Sleep is conventionally characterized as an absence of behavior. But in fact, active (or REM) sleep comprises the paradoxical combination of profound inhibition of muscle tone punctuated by bursts of limb twitching. The causes and functions of these "storms of inhibition and brief whirlwinds of excitation" ([1] p. 560) constitute the central motor mystery of sleep. Until recently, limb twitches were generally considered mere fragments of motor output—generated by a dreaming cerebral cortex—that somehow penetrate the inhibitory medullary barrier that normally prevents us (and other animals) from acting out our dreams [2]. Accordingly, twitching has been considered "at best a caricature of a component of an organized behavioural act" ([3] p. 467) or perhaps "brief episodes of an otherwise integrated behavior that is suppressed by the presence of motor inhibition" ([1] p. 568).

Twitching is among the first behaviors expressed by fetuses [4–6]. In one classic study using fetal rats from embryonic day 16 (E16) through the end of gestation at E20 [4], various categories of spontaneous motor behavior were identified, including localized "convulsive-type jerks and twitches" (p. 101) of the head, mouth, limbs, and tail. These fetal twitches appeared unintegrated, random, and unpredictable. In newborn rats, twitches occur exclusively against a background of muscle atonia, thereby helping to define the state of active sleep before the development of cortical delta activity [7]. Also, twitches are dependent for their expression on the functional integrity of neural circuits within the brainstem's mesopontine region [8, 9]. These and other observations suggest that postnatal twitches are not unintegrated, random, or unpredictable but rather are generated by specific neural structures and are coordinated in time with other components of active sleep.

The common notion that twitches are byproducts of a dreaming cerebral cortex is contradicted by studies showing that twitches appear unaffected by complete disconnection of the forebrain from the brainstem in infant rats [8] and adult cats [10]. Thus, twitches are produced directly and primarily by brainstem neural circuits [2]. Also, contrary to the perception of sleep as a period of relative isolation from peripheral sensory experience, twitches trigger sensory feedback that drives activity in primary somatosensory cortex, thalamus, and hippocampus [11–14]. Given that hundreds of thousands, if not millions, of twitches are produced each day in developing rats, it seems increasingly clear that twitching, like other forms of spontaneous activity in the developing nervous system (e.g., [15–17]), plays a critical role in the development, refinement, and maintenance of sensorimotor circuits in the spinal cord and brain across the lifespan [18–20].

If twitching is indeed a form of spontaneous motor activity that helps to shape the sensorimotor system (while also being shaped by it), then we need to better understand the structure of the limb movements that comprise it, as this structure could serve both as input to sensorimotor learning and a marker of motor organization (e.g., motor synergies). Therefore, the present study aimed to precisely characterize the structure of twitching at individual joints in infant rats and determine whether and how that structure changes over the first postnatal week. Our results provide clear evidence of within- and between-limb synergies at multiple timescales; these synergies exist at birth and are modified lawfully across the early postnatal period. These findings establish twitching as a distinct class of movement and motivate the goal of identifying the behavioral and neural processes underlying activity-dependent development of sensorimotor integration.

*Correspondence: mark-blumberg@uiowa.edu

Please cite this article in press as: Blumberg et al., Spatiotemporal Structure of REM Sleep Twitching Reveals Developmental Origins of Motor Synergies, Current Biology (2013), http://dx.doi.org/10.1016/j.cub.2013.08.055

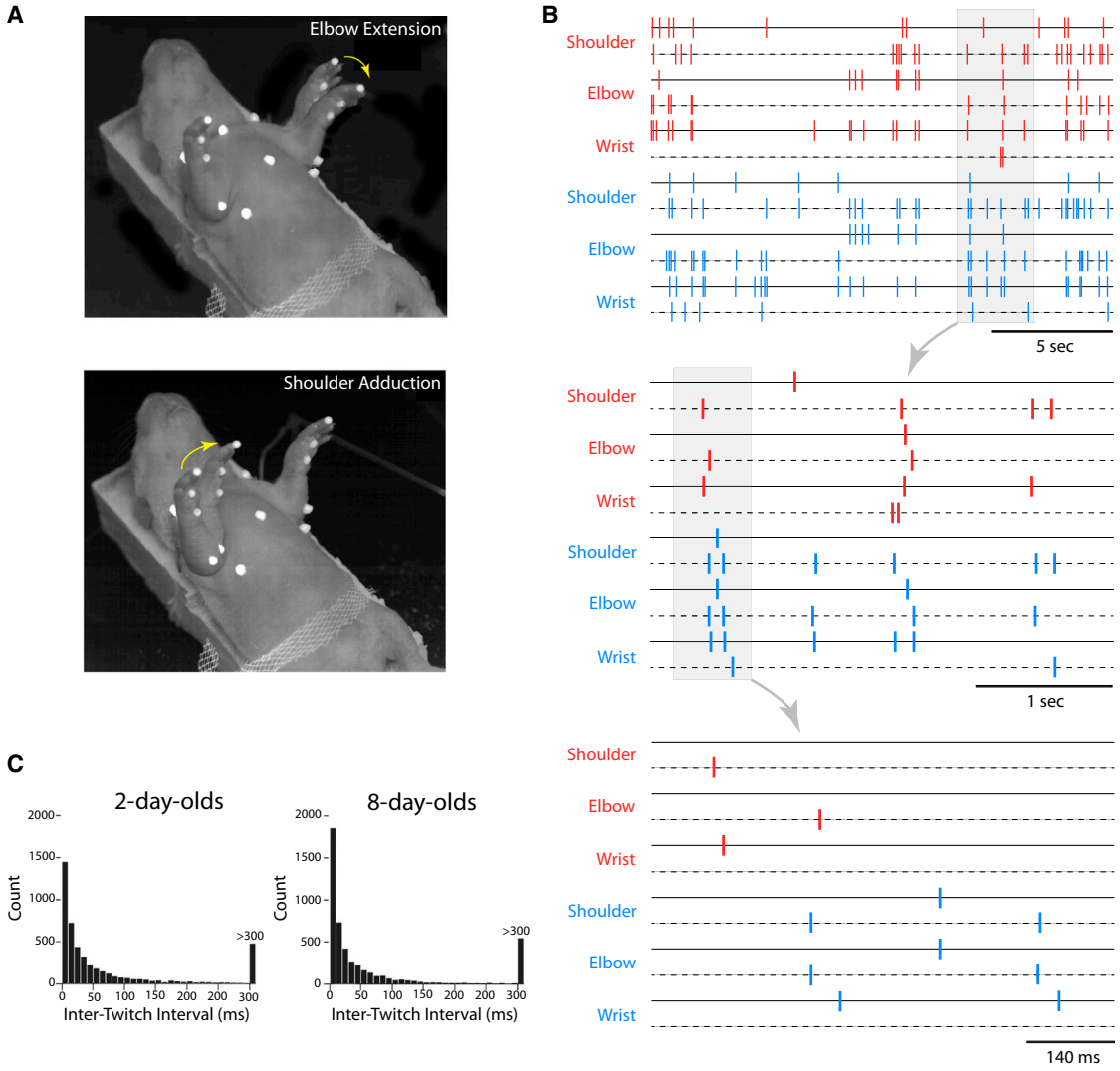

Figure 1. Spatiotemporal Organization of Twitching

(A) Time-lapse photographs, compiled from two sequential high-speed video frames, of a supine 8-day-old rat exhibiting discrete twitches of the left elbow (top) and right shoulder (bottom). Yellow arrows indicate direction of movement. The white dots are used for motion tracking of joint movements.

(B) Spatiotemporal organization of twitching in an 8-day-old rat at three timescales. Each tick mark indicates the occurrence of a twitch in the right (red) or left (blue) forelimb at the shoulder, elbow, or wrist, as determined using high-speed video and motion tracking. For each joint, two movements are depicted: adduction and abduction for the shoulder, and flexion and extension for the elbow and wrist (denoted by solid and dashed lines for each joint). Nonrandom distribution of twitching is evident at each timescale, especially at the two smaller timescales, in which the "bouts-within-bouts" structure of twitching is most apparent.

(C) Frequency distribution of intertwitch intervals for P2 and P8 rats across shoulder, elbow, and wrist joints in the two forelimbs (pooled over >5,000 intervals).

Results

Basic Spatiotemporal Properties of Infant Rat Twitching

We studied twitching in ten P2 and six P8 rats using high-speed video analysis of forelimb twitching and 3D motion tracking. From these rats, a total of 35 and 39 20 s videos were collected, respectively, yielding a total of 4,966 and 5,168 twitches (see Table S1 available online). The number of twitches at individual joints ranged from 228 (right wrist flexion at P2) to 551 (left shoulder adduction at P2; Table S2).

Twitches comprise rapid bursts of activity in multiple limbs, occurring in recognizable bouts with intervening, irregular periods of behavioral quiescence. Twitches at specific joints are often difficult to discern in real time. But, high-speed video of forelimb twitching readily reveals the discrete nature of twitching at the shoulder, elbow, and wrist joints (Figure 1A). Simultaneous twitches at multiple joints are relatively rare, but near-simultaneous twitches of varying complexity, both within and between limbs, are often observed (see Movie S1 for various examples of twitches corresponding to those described above).

A full rendering of a single 20 s video of twitch events across all six joints and joint directions for both forelimbs is shown in the top panel of Figure 1B. At the broadest temporal scale (i.e., 20 s), periods of twitching and interposed periods of quiescence were apparent. At a finer timescale of several seconds (Figure 1B, middle panel), distinct bouts of twitching spanning joints in the two forelimbs were observed. Finally, at an even

Please cite this article in press as: Blumberg et al., Spatiotemporal Structure of REM Sleep Twitching Reveals Developmental Origins of Motor Synergies, Current Biology (2013), http://dx.doi.org/10.1016/j.cub.2013.08.055

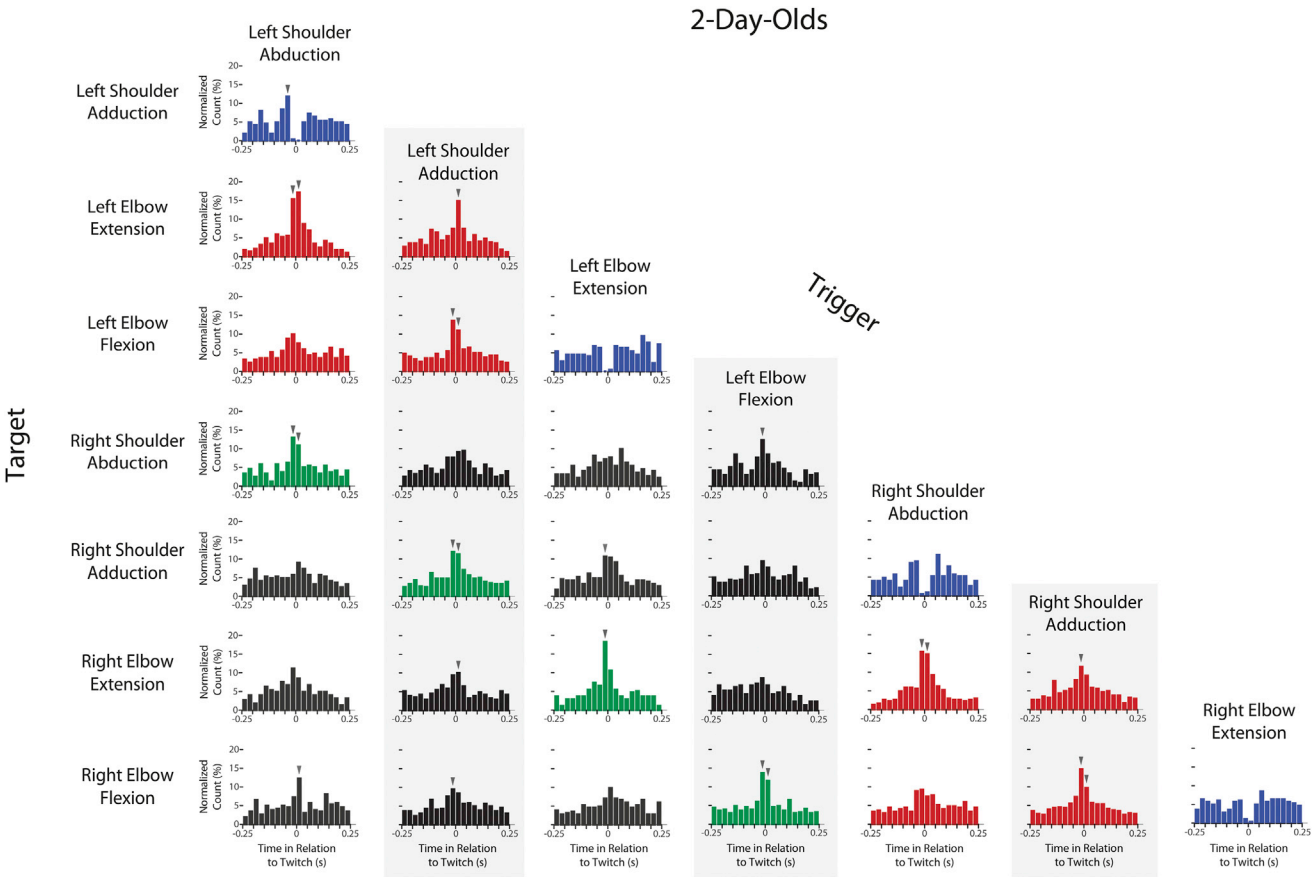

Figure 2. Perievent Histograms Showing the Temporal Pairwise Relations between Twitch Movements at Individual Joints for Infant Subjects at Two Days of Age

For each histogram, the joint movement identified along the left-hand column (i.e., the target) is plotted in relation to the joint movement identified in each column (i.e., the trigger). Because the data were pooled across all 2-day-old subjects, each y axis indicates the total number of target twitches within each 25 ms bin before and after each trigger twitch; these counts are normalized and presented as percentages in relation to the total number of target twitches within the 500 ms histogram window. An arrow above a bin denotes statistical significance at $p < 0.01$. Color shading of plots highlights several categories of movements: across-limb twitches within homologous pairs of movements (green), within-limb synergies (red), and antagonist movements at the same joints (blue). Data for wrist movements are not shown.

finer timescale of less than 1 s (Figure 1B, bottom panel), additional bouts of twitching were revealed. This "bouts-within-bouts" temporal structure was typical.

As shown in Figure 1C for P2 and P8 subjects, the majority of intertwitch intervals were shorter than 100 ms, thus roughly defining the temporal boundaries of a twitch bout at these ages. However, the bouts-within-bouts structure of twitching cautions against the expectation of a single boundary that distinguishes twitching bouts at all scales [21]. Indeed, twitching might be better characterized as a hierarchically organized structure comprising sets of partially overlapping events.

The analyses described below focus only on shoulder and elbow movements. We excluded wrist movements because they had smaller amplitudes than shoulder and elbow movements, making it harder to detect them independently, especially when other joints were moving.

Pairwise Temporal Relations of Twitching at Individual Joints

Figures 2 and 3 show perievent histograms that capture the temporal relations within pairs of joint movements for P2 and P8 subjects, respectively. Each histogram indicates the total number of target events that co-occurred with the trigger event (at time 0) within each 25 ms time bin around the trigger. At both P2 and P8, there were many instances of significant coexpression of joint movements. For example, consider the four types of homologous twitches of the right and left forelimbs (e.g., right and left shoulder adduction, highlighted in green; see Movie S1). In all four instances, a twitch in one forelimb was likely to be preceded or succeeded within 25 ms by a homologous twitch in the other forelimb. Similarly, for pairwise movements within a forelimb (e.g., left shoulder adduction and left elbow flexion; highlighted in red), movements most often occurred within 25 ms of each other (the exception being the relatively weak relations between elbow flexions and shoulder abductions). Finally, although antagonist movements (e.g., elbow flexion and extension; highlighted in blue) could not physically occur at the same time, they did co-occur within a 100 ms window and were more strongly expressed at P8 than at P2.

Age-Related Changes in Twitching

To statistically confirm the observations above and determine how twitching changes over development, we created

Please cite this article in press as: Blumberg et al., Spatiotemporal Structure of REM Sleep Twitching Reveals Developmental Origins of Motor Synergies, Current Biology (2013), http://dx.doi.org/10.1016/j.cub.2013.08.055

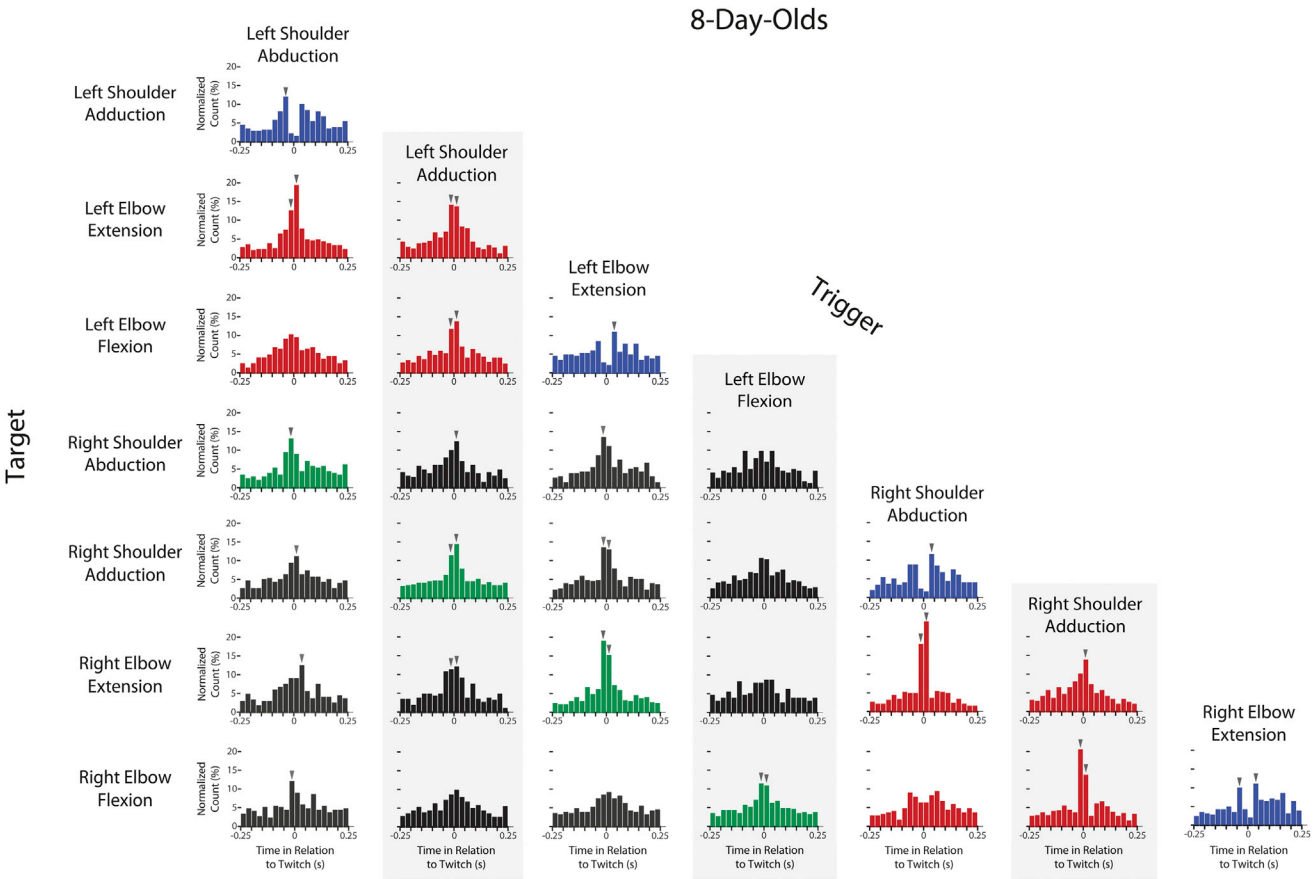

Figure 3. Perievent Histograms Showing the Temporal Pairwise Relations between Twitch Movements at Individual Joints for Infant Subjects at Eight Days of Age

Details are identical to those described for Figure 2.

a "windowed data set." We constructed this data set by stepping through the raw data in 100 ms increments and identifying the twitches that occurred within each of these windows (or events; see Supplemental Experimental Procedures). Only events with at least two twitches were included.

Figure 4A shows the proportion of events containing twitches at homologous joints in the left and right forelimbs at P2 and P8. An age (2) × joint (4) mixed ANOVA revealed no main effect of age ($F [1, 11] < 1$, NS) but a significant main effect of joint ($F [3, 33] = 12.0$, $p < 0.001$) and a significant joint × age interaction ($F [3, 22] = 4.3$, $p < 0.05$). Thus, there are age-related changes in the coexpression of homologous twitches across the two limbs, but the effect of age is not unidirectional.

We next assessed the relative occurrence of homologous and nonhomologous twitches. We limited this analysis (and this analysis only) to the subset of events in which there were only two twitches, one on each side of the body (P2, 46.1 events/pup; P8, 35.2 events/pup). Within these events, we classified (for each joint) whether the events were homologous (e.g., left and right shoulder adduction) or nonhomologous (e.g., left shoulder adduction and right shoulder abduction). The results (Figure 4B) show that homologous movements at the shoulder and elbow were more likely than nonhomologous movements. A joint (shoulder/elbow) × twitch-type (homologous/nonhomologous) × age ANOVA indicated that there was no main effect of joint ($F [1, 11] < 1$) or age ($F [1, 11] = 1.9$, NS). However, the main effect of twitch type was significant ($F [1, 11] = 14.2$, $p = 0.003$), and this did not interact with joint or age. Overall, homologous twitches (mean = 0.38 ± 0.03) were about 1.7 times more prevalent than nonhomologous twitches (mean = 0.22 ± 0.03).

We next examined antagonist movements within a joint (Figure 4C). A joint × age ANOVA revealed significant main effects of joint movement ($F [1, 11] = 8.5$, $p < 0.05$) and age ($F [1, 11] = 6.1$, $p < 0.05$) but no joint movement × age interaction ($F [1, 11] = 2.8$, NS). This age-related increase in antagonist twitches at both joints is consistent with the perievent histograms presented in Figures 2 and 3 (highlighted in blue).

Finally, as a prelude to the next analyses of twitching across more than two joints, we examined the proportion of events containing two or more twitches (Figure 4D). A twitch count × age ANOVA revealed significant main effects of number of twitches per event ($F [3, 22] = 369.8$, $p < 0.001$) and age ($F [1, 11] = 11.3$, $p < 0.01$), and a significant twitch count × age interaction ($F [3, 22] = 9.2$, $p < 0.001$). There were more twitch movements within the same 100 ms windows at P8 than at P2 (i.e., larger proportions of four- and five-twitch events, and fewer two-twitch events), suggesting that twitching becomes more complex with age. A follow-up analysis using Monte Carlo randomizations indicated that at both ages, three-, four-, and five-twitch events were more likely than expected by chance, whereas two-twitch events were not (Figure S1).

Please cite this article in press as: Blumberg et al., Spatiotemporal Structure of REM Sleep Twitching Reveals Developmental Origins of Motor Synergies, Current Biology (2013), http://dx.doi.org/10.1016/j.cub.2013.08.055

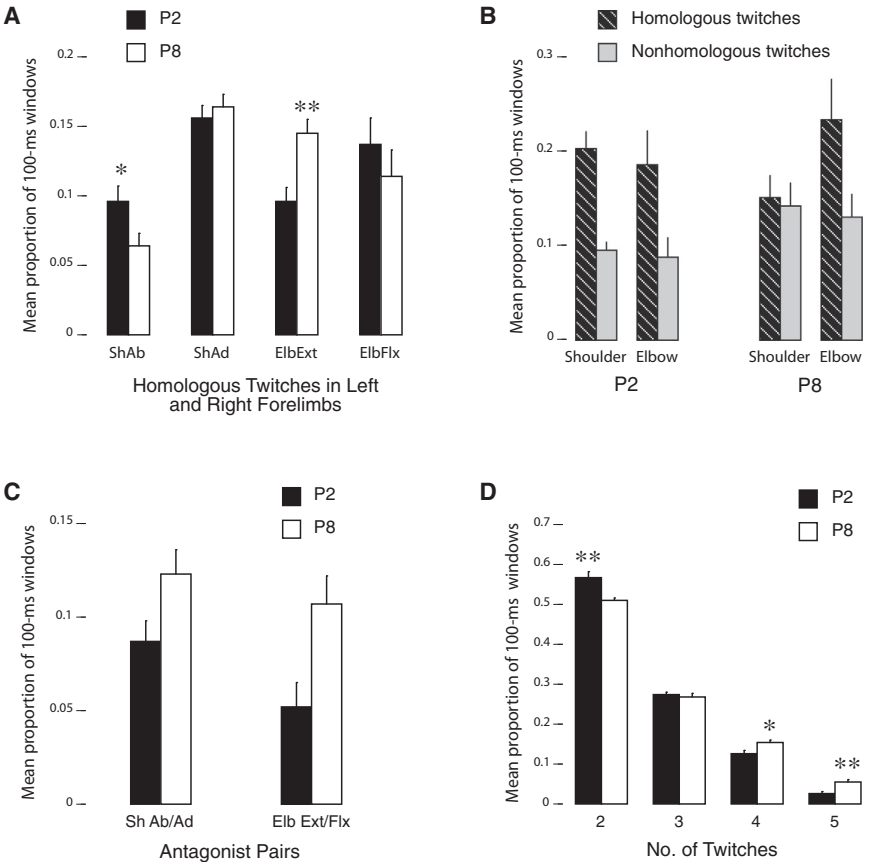

Figure 4. Quantitative Differences in Twitching

(A) Mean proportion of 100 ms windows (per pup/litter) containing antagonist twitch movements at the shoulder (adduction and abduction) and elbow (flexion and extension) at P2 (black bars) and P8 (white bars).

(B) Mean proportion of 100 ms windows containing homologous (striped bars) or nonhomologous (gray bars) twitch movements at the left and right shoulder or elbow at P2 and P8. For this analysis, only those windows containing two movements, one on each side of the body, were included.

(C) Mean proportion of 100 ms windows containing twitches at homologous joints in the left and right forelimbs at P2 (black bars) and P8 (white bars).

(D) Mean proportion of 100 ms windows containing two, three, four, or five twitches at P2 (black bars) and P8 (white bars). See Figure S1 for a corresponding analysis in relation to chance. Events containing zero and one twitches were excluded from this analysis. All data are means + SE. Abbreviations are as in Figure 2. n = 7 (P2) and 6 (P8). *$p < 0.05$, **$p < 0.01$.

Hierarchical Cluster Analysis Reveals Complex Spatiotemporal Structure of Twitching

To determine whether twitching exhibits complex structure among more than two joints, we performed hierarchical cluster analysis (HCA) with seriation separately on the windowed data set at P2 and P8 [23]. Unlike traditional HCA, this analysis simultaneously extracts structure on two dimensions: clusters among the limbs (the dendrograms at the top of Figure 5) and clusters among the events (the rotated dendrograms on the sides). By extracting clusters on two dimensions simultaneously, seriation provides a more powerful way to visualize structure in complex data sets. For comparison, we performed identical analyses using randomized data sets (Figure S2).

The dendrograms describing clustering among limbs (Figure 5, top clusters) exhibit clear functional structure. At both ages, shoulder abductions are tightly clustered with elbow extensions within each of the left and right forelimbs (green and purple branches). In contrast, we observed a developmental change in shoulder adductions and elbow flexions: at P2 the primary clustering occurs for homologous twitches on different sides (i.e., right/left shoulder adduction, right/left elbow flexion), whereas at P8 this shifts to complementary twitches within a side (i.e., shoulder adduction and elbow flexion). It is important to note, however, that at the second level of clustering these four joints movements are grouped similarly at both ages, suggesting that the observed age-related change does not represent a complete reorganization but rather a shift in the prominence of within- versus between-limb structure. In short, all low-level clusters at P8 exhibit within-limb linkages, with higher-level clusters linking homologous twitches across the two limbs. In contrast, the linkages at P2 are less systematic.

Although HCA provided a clear picture of structure among twitches, it offered a more complex picture of structure among events (Figure 5, rotated dendrograms). This is crucial: in addition to wanting to know, for example, that right elbow extensions are closely linked with right shoulder abductions, we also want to know if there were specific types of twitch movements that co-occurred. The rotated clusters suggest a wide variety of multitwitch patterns with a complex overlapping structure. For example, in Figure 5A, the yellow box highlights one region (a group of events) in which right elbow extensions are often linked with right shoulder abductions (the top half of this region); however, just below it is a cluster of events illustrating a linkage between the same right elbow extension and a left elbow extension (homologous twitches). These linkages contribute to the first two cluster levels observed in this region. However, within this region there are also clusters illustrating weaker linkages between the right elbow extension and left shoulder abduction (also contributing to the second-level clustering) as well as a smattering of other joint movements. This complexity suggests that twitching at any given time reflects the overlapping influence of multiple movement patterns. Whereas HCA can only link each event to a single cluster, if events were probabilistically assignable to more than one cluster, a more coherent structure might emerge. To move beyond this limitation we turned to latent class analysis.

Latent Class Analysis Reveals the Development of Complex Multijoint Patterns of Twitches

Latent class analysis (LCA) was performed separately on the windowed data set at P2 and P8, yielding 28 clusters at P2 and 21 clusters at P8. Of these, 19 clusters at P2 and 16 clusters at P8 showed contributions from three or more joints, further supporting the multijoint structure of twitching (see

Please cite this article in press as: Blumberg et al., Spatiotemporal Structure of REM Sleep Twitching Reveals Developmental Origins of Motor Synergies, Current Biology (2013), http://dx.doi.org/10.1016/j.cub.2013.08.055

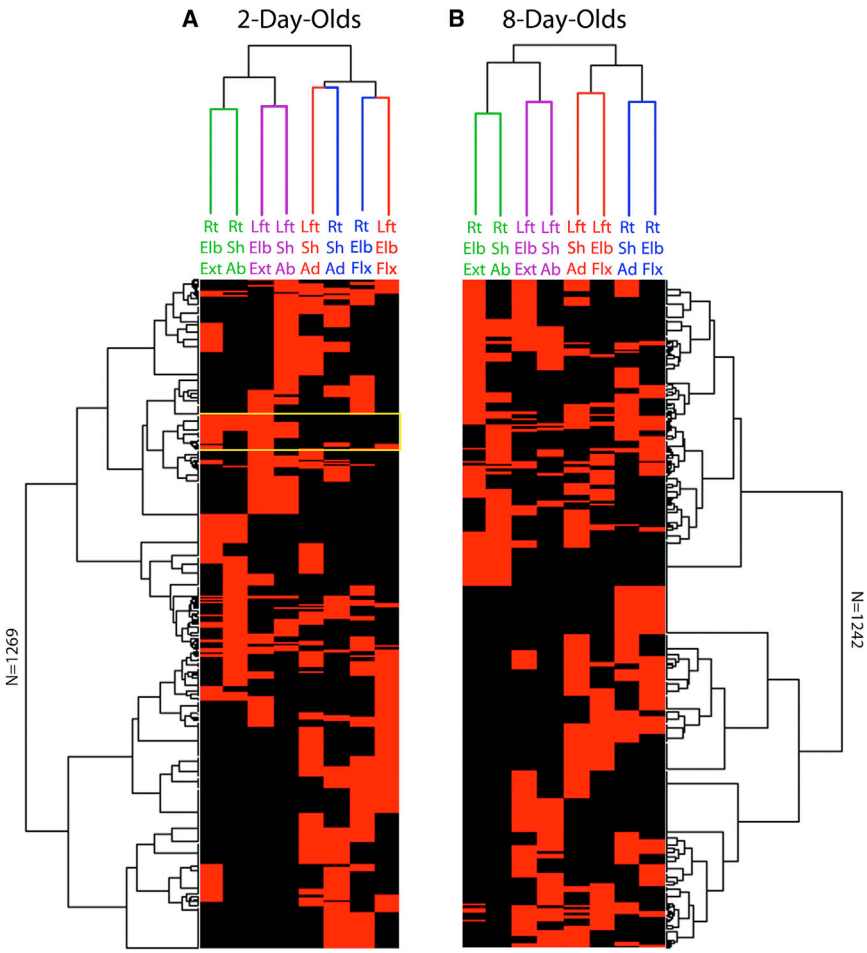

Figure 5. Hierarchical Cluster Analyses, with Seriation, of Multijoint Twitches at the Shoulder and Elbow of Both Forelimbs

These analyses were performed on the 100 ms windowed data set. Each row of data flows vertically down each figure, with red corresponding to the presence of a twitch and black to its absence. There are a total of 1,269 rows (or events) at 2 days of age (A) and 1,242 rows at 8 days of age (B). In addition to the dendrograms depicted at the top of each figure depicting relationships among the joints, seriation is used to produce the dendrograms along the rows to reveal structure among the events in the data. The color coding for the dendrograms at the top highlights similar and dissimilar clustering at the two ages. The yellow box is discussed in the text. For comparison with randomized data, see Figure S2. Abbreviations: Rt, right; Lft, left; Sh, shoulder; Elb, elbow; Ad, adduction; Ab, abduction; Flx, flexion; Ext, extension.

Figure S1). LCA provides a set of profile plots for each cluster, with each plot showing how strongly particular twitch movements are associated with that cluster. Each profile plot was initially examined visually to assess the degree to which similar twitch patterns occurred at P2 and P8. Noting many instances of similar profile plots, we devised an objective method to match specific clusters across ages (see Supplemental Experimental Procedures). In total, 18 matched clusters were identified and nearly all of these were also identified during our initial visual inspection.

Eight representative pairs of matched clusters are shown in Figure 6. Many of the matched clusters comprised twitches at two joints within the same limb (e.g., shoulder adduction and elbow flexion; Figure 6A). However, other matched clusters were transformed from two-joint between-limb movements at P2 into more complex multijoint limb movements at P8 with additional joints added on a partial basis (Figure 6B, top two rows). But no single pattern describes all changes in clusters between P2 and P8 (Figure 6B, bottom two rows).

We conducted a regression analysis to determine whether there were subtler shifts over development. We focused on two key measures for each cluster (at each age): frequency of occurrence and coherence. To measure the coherence of a cluster, we computed each cluster's Shannon entropy, which measures the degree of structure in the twitches. Here, random clusters (e.g., with all limbs involved to some degree) will have higher entropies, and clusters with a smaller number of frequently occurring twitches will have lower entropies (see Supplemental Experimental Procedures).

To determine how cluster frequency and entropy change over time, regression analyses were performed on cluster frequency (log transformed) and entropy at P2 and P8. Figures 7A and 7B show that within each age, there were no significant relationships between cluster frequency and entropy (P2: $r^2 = 0.13$, $\beta = -0.32$, $F\,[1, 16] = 2.3$, NS; P8: $r^2 = 0.04$, $\beta = -0.17$, $F\,[1, 16] < 1$, NS; vertical arrows in Figures 7E and 7F). That is, higher frequency clusters were not more or less coherent at either age. Similarly, there was moderate stability in a cluster's entropy between P2 and P8 ($r^2 = 0.34$, $\beta = 0.59$, $F\,[1, 16] = 8.3$, $p < 0.05$; lower horizontal arrows in Figures 7E and 7F). This was expected since clusters were matched across ages using the same probabilities over which their entropies were computed. There was also stability in a cluster's frequency between P2 and P8 ($r^2 = 0.25$, $\beta = 0.50$, $F\,[1, 16] = 5.3$, $p < 0.05$; upper horizontal arrows in Figures 7E and 7F).

Quite strikingly, however, P2 cluster frequency was significantly related to cluster entropy at P8 ($r^2 = 0.45$, $\beta = -0.58$, $F\,[1, 16] = 12.8$, $p < 0.005$; Figure 7C, diagonal in Figure 7E). This was true even after partialing out P8 cluster entropy (the same-age correlation) and P2 cluster entropy (the autocorrelation) in a hierarchical regression (Figure 7E, diagonal path; $r^2_{\Delta} = 0.37$, $F\,[1, 14] = 20.1$, $p < 0.001$).Thus, higher-frequency clusters at P2 became more highly organized (lower entropy) clusters at P8. This suggests that with "practice," the animal prunes secondary movements from the cluster.

Conversely, P2 cluster entropy predicted cluster frequency at P8 ($r^2 = 0.33$, $\beta = -0.57$, $F\,[1, 16] = 7.8$, $p < 0.05$). Here, more organized (lower entropy) clusters at P2 became more frequent clusters at P8 (Figure 7D, diagonal in Figure 7F). Again, this effect was confirmed over and above the effect of cluster entropy at P8 (the same-age correlation) and cluster frequency at P2 (the autocorrelation) in a hierarchical regression (Figure 7F; $r^2_{\Delta} = 0.36$, $F\,[1, 14] = 14.1$, $p < 0.005$).

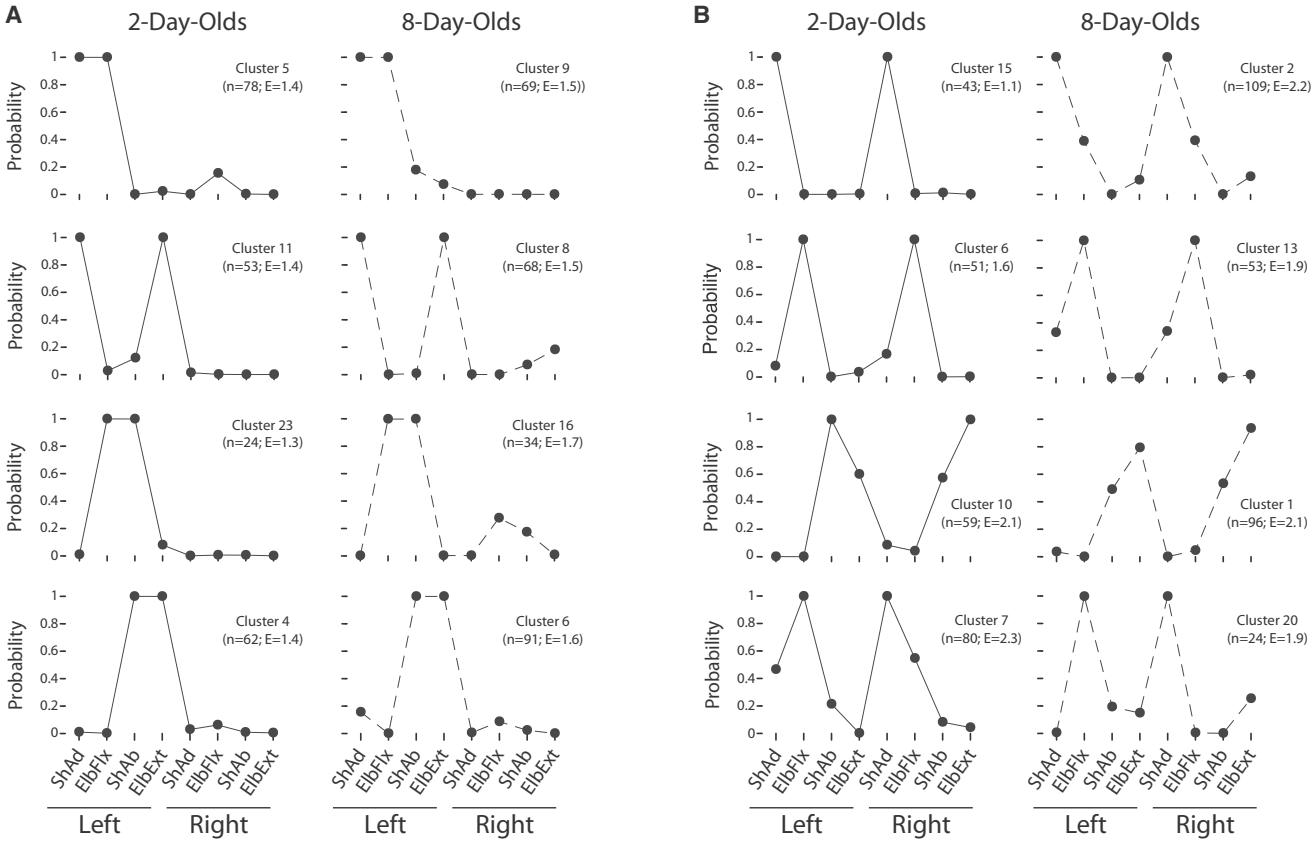

Figure 6. Profile Plots of Multijoint Patterns of Twitching Identified Using Latent Class Analysis

As in the hierarchical cluster analysis presented in Figure 5, the latent class analysis (LCA) was performed using the 100 ms windowed data set. In total, 28 clusters were identified at 2 days of age and 21 clusters were identified at 8 days of age. Subsequently, we used two methods to match similar clusters at the two ages (see Supplemental Experimental Procedures); only the profile plots for matched clusters are presented in the figure (out of a total of 18 matched clusters). Each plot can be interpreted as the likelihood that, given the existence of a cluster, a particular joint movement would be included within it. The figure presents a sampling of profile plots for clusters comprised primarily of movements at two joints (A) and more than two joints (B). For each cluster, its frequency (n) and entropy (E) are shown. Abbreviations: ShAd, shoulder adduction; ElbFlx, elbow flexion; ShAb, shoulder abduction; ElbExt, elbow extension.

Discussion

Twitches have long been considered mere jetsam of a dreaming brain—unstructured and largely unnoticed fragments of behavior [2]. In contrast, the present results indicate that twitches are highly structured behaviors and suggest that they provide functionally meaningful content for the developing nervous system. These results are surprising in light of prior research. For example, a seminal study of behavior in rat fetuses [4], discussed above, failed to find evidence of interlimb coordination. Specifically, at E16 (i.e., 5 days before birth) the right and left forelimbs were "not mirror-imaged or otherwise coordinated" (p. 106) and at E19 still "no coordination of left and right [fore]limbs was detected" (p. 108). In a subsequent investigation, Robinson et al. [6] provided evidence of bout structure from E17 through P9; however, they did not find evidence of complex patterns across joints or limbs, such as multijoint movements within a limb. As they noted, however, this failure could have resulted from the limitations of the conventional video methods used in their study.

By using high-speed video and 3D reconstruction of movements at individual forelimb joints, we more accurately assessed the content of twitching and how it changes across the first postnatal week. Our results reveal—within and across limbs—heretofore undetected and unexpected complex spatiotemporal structure that is expressed over multiple timescales and modified lawfully across age. The motor synergies inherent in twitching provide clues to the underlying neural circuitry generating these movements and point toward possible mechanisms of sensorimotor development.

Brainstem and Spinal Circuits May Contribute to Twitching at Different Timescales

What neural mechanisms underlie the patterns of twitching observed here, including the bouts-within-bouts structure? One possibility is that the spatiotemporal structure of twitching arises from spinal circuits alone, as may be the case at E20 [6]. However, disrupting midbrain circuits during the first postnatal week significantly affects the expression of twitching [8, 24]. Moreover, given that twitching at P2 is tightly coupled with muscle atonia, brainstem mechanisms must already be coordinating sleep components at this age (see [7]). Thus, the neural control of twitching appears to migrate from autonomous spinal control in fetuses to substantial brainstem control early in postnatal development.

It may be that limb twitches are produced by a combination of spinal mechanisms interacting with descending brainstem motor systems, including the rubrospinal, vestibulospinal, and reticulospinal pathways [25]. Each of these pathways contributes differentially to the control of skeletal muscles and

Please cite this article in press as: Blumberg et al., Spatiotemporal Structure of REM Sleep Twitching Reveals Developmental Origins of Motor Synergies, Current Biology (2013), http://dx.doi.org/10.1016/j.cub.2013.08.055

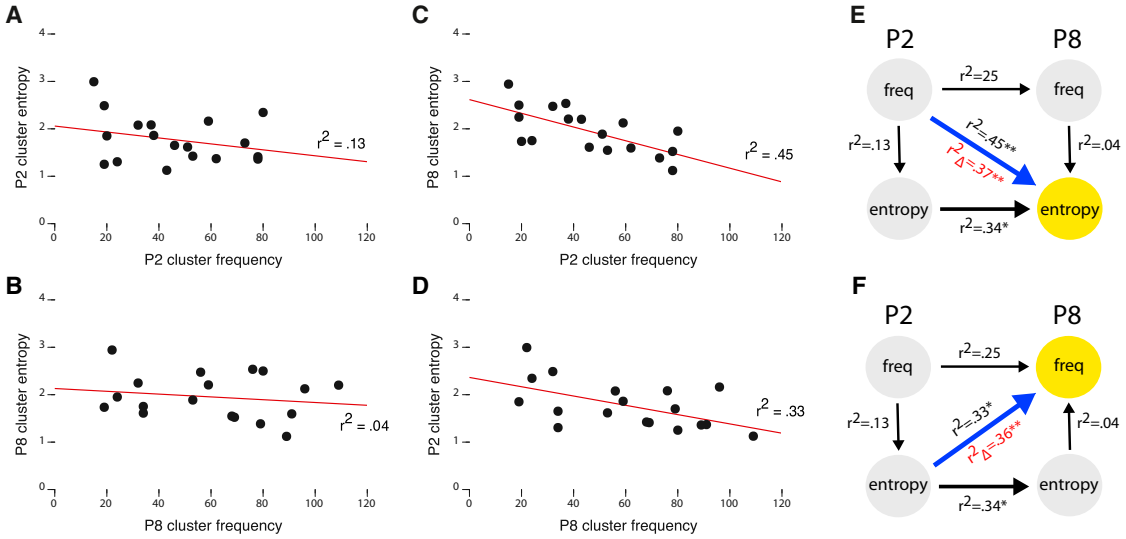

Figure 7. Regression Analyses of the Relations between Cluster Frequency and Entropy

(A–D) Using the frequency and entropy values for only the matched clusters identified using LCA (see Figure 5), linear regression analyses were performed. At P2 (A) and P8 (B), cluster frequency is unrelated to cluster entropy. However, as shown in (C), clusters that were more frequent at P2 became clusters with lower entropy at P8. Conversely, as shown in (D), clusters that were more frequent at P8 were the clusters with lower entropy at P2.

(E) Hierarchical regression analysis with entropy at P8 as the dependent variable (yellow circle) reveals that cluster frequency at P2 significantly accounts for the variance in entropy at P8 (blue arrow), over and above the effects of cluster entropy at P2 and cluster frequency at P8 (r^2_Δ, in red).

(F) Hierarchical regression analysis with frequency at P8 as the dependent variable (yellow circle) reveals that cluster entropy at P2 significantly accounts for the variance in cluster entropy at P8 (blue arrow), over and above the effects of cluster frequency at P2 and cluster entropy at P8 (r^2_Δ, in red). *p < 0.05, **p < 0.005.

could therefore contribute to twitching. Some evidence for this comes from neurophysiological recordings in the red nucleus—the source of the rubrospinal tract—in adult cats [26]; red nucleus activity increased phasically during active sleep, especially just before rapid eye movements and myoclonic twitches. However, lesions to the red nucleus did not disrupt the quantity or patterning of twitching. Unfortunately, from these and other studies (e.g., [3]), we still lack definitive information about the relative contributions of descending motor systems to limb twitching in adults; even less is known about these systems early in development.

Leaving aside the specific brainstem pathways, the bouts-within-bouts structure could arise from different neural components contributing at different timescales. For example, a brainstem signal could initiate a bout of twitching and, in doing so, trigger a cascade of subsequent twitches that are structured and/or mediated by spinal mechanisms. What kinds of spinal mechanisms might be involved in this process? One possibility is that a twitching limb, via proprioceptive or tactile feedback, triggers additional twitches via reflexes. However, in adult cats, monosynaptic and polysynaptic spinal reflexes are powerfully inhibited during periods of twitching [27–29]. Indeed, without these inhibitory mechanisms, one wonders what would stop a twitch from reverberating (e.g., between agonist and antagonist movements at a single joint). Regardless, it is not known whether these inhibitory mechanisms are functional in early infancy.

A second and more likely possibility is that a descending signal to a spinal motoneuron triggers a twitch and also activates, in parallel, additional components of spinal circuitry. For example, consider the strong propensity for homologous twitches to occur in the left and right forelimbs (e.g., Figure 4B). Although such patterns could be produced by bilaterally descending twitch-production nuclei in the brainstem, they could also reflect the action of commissural interneurons (CINs) [30]. CINs, which are functional in newborn mice [31], coordinate synchronous and alternating limb movements through excitatory or inhibitory actions on spinal motoneurons controlling functionally similar muscles on the two sides of the body. Accordingly, the homologous pattern of twitching could arise from a combination of descending brainstem activation of spinal motoneurons and their associated CINs, followed in succession by the activation of motoneurons in the contralateral spinal cord. Similar intrinsic spinal circuits, including those controlling flexor-extensor movements at the same joint [30], could contribute to other twitch patterns that we observed. Finally, the combined actions of spinal circuit activation and sensory feedback from twitching could contribute to the development, refinement, and maintenance of these functional spinal circuits.

Solving Bernstein's Problem in Our Sleep: Twitching, Motor Synergies, and Exploratory Behavior

The discovery of motor synergies expressed within the context of sleep suggests that twitching is a form of exploratory movement that contributes to the development of goal-directed behaviors like reaching. With regard to such movements, Nikolai Bernstein classically described the challenge of selecting a single movement trajectory from a wide array of possible trajectories [32]. One of his solutions to this so-called degrees-of-freedom problem was to propose motor synergies as the functional units of motor planning. As Sporns and Edelman summarize Bernstein's perspective, "synergies are used by the developing nervous system to reduce the number both of controlled parameters and of afferent signals needed to generate and guide ongoing movement" ([33] p. 963). Motor control theorists continue to elaborate upon Bernstein's concepts and propose new solutions to the degrees-of-freedom problem [22].

In attempting to understand how human infants solve Bernstein's problem, developmental psychologists have focused on exploratory behavior as a key contributor to the emergence of goal-directed behaviors [33–37]. As but one example, Sporns and Edelman proposed a solution in which "somatic selection of neuronal groups" leads to the "progressive transformation of a *primary movement repertoire* into a set of motor synergies and adaptive action patterns" ([33] p. 960, italics added). Our results also suggest a selectionist process whereby certain motor synergies, based on their prevalence and structure, are retained and elaborated across the first postnatal week during sleep (Figure 7). These nascent synergies could form at least part of the primary movement repertoire of the developing infant from which more complex movements are built. Therefore, in contrast to most conceptions of motor development, our results introduce a nonobvious factor in building movement repertoires. Accordingly, motor practice and exploration need not be restricted to waking movements. Instead, the enormous quantity of twitches produced by the sleeping infant may provide critical early experiences that help shape and refine motor synergies and perhaps even contribute to the development of so-called "motor primitives" [38].

Twitching may also help the animal develop more precise expectations of the sensorimotor consequences of an action. By generating a movement and observing its proprioceptive consequences—including sensory consequences arising from passively moving joints—the animal can learn kinematic and biomechanical relationships among muscles, joints, and effectors and their perceptual correlates [18, 35, 39, 40], much as "motor babbling" may help an animal learn the visual consequences of an action [41]. In that sense, the particular co-occurrence patterns embedded in the twitch events could prepare the organism to perceive the consequences of highly likely multijoint actions.

Additional clues to the functions of twitching are starting to emerge from developmental robotics, an interdisciplinary field that is shifting our understanding of how development contributes to the emergence of flexible and adaptable behavior [42]. Specifically, in a robotic or simulated limb equipped with joints, muscles, and sensors, a training regimen comprising unstructured and intermittent "twitches" of the synthetic muscles resulted in discrete movements of the joints and distinct sensory responses conveying force and stretch information to the "nervous system" [18, 40]. Incredibly, even just a brief regimen of twitching resulted in the self-organization of spinal reflexes, including stretch and withdrawal reflexes.

Developmental changes in the patterns of twitching suggest experience-based pruning of organization: although twitching might initially be unstructured (e.g., in fetal rats), over time, the more prevalent patterns are refined and the less refined patterns are eliminated. This selectionist process is broadly consistent with what is known about development in many other domains including speech perception [43], mathematical reasoning [44], face perception [45], and word learning [46]. In many of these cases, Hebbian and anti-Hebbian processes have been posited as mechanisms of self-organization [44, 46]; similar processes could be at play with respect to the developmental consequences of twitching [18].

Conclusions

Sensory feedback from twitches exerts a powerful influence over infant nervous system activity, from spinal cord [20] to forebrain [11–14]. The present results close the loop by showing that the structure of twitching evolves over time, suggesting that developmental experience—including sensory feedback from twitches—modifies the neural structures that produce subsequent twitches. Delineating this process of feedback modulation and sensorimotor integration remains a future challenge, as does resolving the contributions of twitching to other aspects of activity-dependent development—from synapse formation and elimination to topographic organization [18].

The multijoint patterning of twitching at P2 and its modification across the first postnatal week suggests that twitching is part of a learning system whereby basic motor synergies are retained and refined, or eliminated. In time, these motor synergies might be automatized and flexibly linked with other synergies to produce the more complex patterns of behavior that characterize waking life. There is as yet little information concerning the structural and functional relations among twitching and waking movements (e.g., locomotion [47]) in healthy subjects of any age or species. However, a recent investigation of motor behavior in human adults with REM sleep behavior disorder should encourage more work in this area [48]. Regardless, the present findings highlight twitching—arguably the most prevalent behavior of early infancy in rats and other mammals—as an unexpected form of coordinated behavior that could provide useful insights to scientists and clinicians about the functional status of the healthy and damaged nervous system across the lifespan.

Experimental Procedures

Subjects

Subjects were male and female Sprague-Dawley Norway rats (*Rattus norvegicus*). A total of ten P2 rats from seven litters (body weight 6.1–8.2 g) and six P8 rats from six litters (body weight 17.2–20.1 g) were used. Experiments were carried out in accordance with the National Institutes of Health Guide for the Care and Use of Laboratory Animals (NIH publication number 80-23) and were approved by the Institutional Animal Care and Use Committee of the University of Iowa.

High-Speed Video Recording and Data Acquisition

A pup was secured in a supine position inside a humidified incubator maintained at thermoneutrality. When the pup was cycling between sleep and wakefulness, two high-speed digital video cameras were used to record twitching behavior. During each 20 s recording period, the experimenter closely monitored the pup and confirmed that only twitches were expressed. Multiple 20 s recordings were acquired from each pup.

Data Reduction and Analysis

Automatic motion tracking was supplemented by frame-by-frame confirmation and, when necessary, manual correction. We identified six joint angles or line distances that reliably identified shoulder abduction and adduction, elbow extension and flexion, and wrist extension and flexion. These angles and distances were converted to discrete twitch events indicating movement onset times for the six joints across the two forelimbs. Because of the short duration of each individual 20 s recording, most analyses were performed on pooled data at each age. These pooled data sets were used for the analyses performed here.

Supplemental Information

Supplemental Information includes two figures, two tables, Supplemental Experimental Procedures, and one movie and can be found with this article online at http://dx.doi.org/10.1016/j.cub.2013.08.055.

Acknowledgments

Preparation of this article was made possible by National Institutes of Health research grants to M.S.B. (HD63071) and B.M. (DC008089) and an Independent Scientist Award to M.S.B. (MH66424). We thank Roger Bakeman,

Magnus Magnusson, and Kristian Markon for analytical assistance; Josie Delgado for technical assistance; and Hugo Gravato Marques for helpful comments on an earlier draft of the paper.

Received: July 23, 2013
Revised: August 21, 2013
Accepted: August 22, 2013
Published: October 17, 2013

References

1. Chase, M.H., and Morales, F.R. (1990). The atonia and myoclonia of active (REM) sleep. Annu. Rev. Psychol. *41*, 557–584.
2. Blumberg, M.S. (2010). Beyond dreams: do sleep-related movements contribute to brain development? Front. Neurol. *1*, 140.
3. Gassel, M.M., Marchiafava, P.L., and Pompeiano, O. (1964). Phasic changes in muscular activity during desynchronized sleep in unrestrained cats. An analysis of the pattern and organization of myoclonic twitches. Arch. Ital. Biol. *102*, 449–470.
4. Narayanan, C.H., Fox, M.W., and Hamburger, V. (1971). Prenatal development of spontaneous and evoked activity in the rat (Rattus norvegicus albinus). Behaviour *40*, 100–134.
5. Corner, M.A. (1977). Sleep and the beginnings of behavior in the animal kingdom—studies of ultradian motility cycles in early life. Prog. Neurobiol. *8*, 279–295.
6. Robinson, S.R., Blumberg, M.S., Lane, M.S., and Kreber, L.A. (2000). Spontaneous motor activity in fetal and infant rats is organized into discrete multilimb bouts. Behav. Neurosci. *114*, 328–336.
7. Blumberg, M.S., and Seelke, A.M.H. (2010). The form and function of infant sleep: From muscle to neocortex. In The Oxford Handbook of Developmental Behavioral Neuroscience, M.S. Blumberg, J.H. Freeman, and S.R. Robinson, eds. (New York: Oxford University Press), pp. 391–423.
8. Kreider, J.C., and Blumberg, M.S. (2000). Mesopontine contribution to the expression of active 'twitch' sleep in decerebrate week-old rats. Brain Res. *872*, 149–159.
9. Karlsson, K.Æ., Gall, A.J., Mohns, E.J., Seelke, A.M.H., and Blumberg, M.S. (2005). The neural substrates of infant sleep in rats. PLoS Biol. *3*, e143.
10. Villablanca, J. (1966). Behavioral and polygraphic study of "sleep" and "wakefulness" in chronic decerebrate cats. Electroencephalogr. Clin. Neurophysiol. *21*, 562–577.
11. Khazipov, R., Sirota, A., Leinekugel, X., Holmes, G.L., Ben-Ari, Y., and Buzsáki, G. (2004). Early motor activity drives spindle bursts in the developing somatosensory cortex. Nature *432*, 758–761.
12. Mohns, E.J., and Blumberg, M.S. (2010). Neocortical activation of the hippocampus during sleep in infant rats. J. Neurosci. *30*, 3438–3449.
13. Tiriac, A., Uitermarkt, B.D., Fanning, A.S., Sokoloff, G., and Blumberg, M.S. (2012). Rapid whisker movements in sleeping newborn rats. Curr. Biol. *22*, 2075–2080.
14. McVea, D.A., Mohajerani, M.H., and Murphy, T.H. (2012). Voltage-sensitive dye imaging reveals dynamic spatiotemporal properties of cortical activity after spontaneous muscle twitches in the newborn rat. J. Neurosci. *32*, 10982–10994.
15. Wong, R.O. (1999). Retinal waves and visual system development. Annu. Rev. Neurosci. *22*, 29–47.
16. Spitzer, N.C. (2006). Electrical activity in early neuronal development. Nature *444*, 707–712.
17. Tritsch, N.X., Yi, E., Gale, J.E., Glowatzki, E., and Bergles, D.E. (2007). The origin of spontaneous activity in the developing auditory system. Nature *450*, 50–55.
18. Blumberg, M.S., Marques, H.G., and Iida, F. (2013). Twitching in sensorimotor development from sleeping rats to robots. Curr. Biol. *23*, R532–R537.
19. Khazipov, R., and Luhmann, H.J. (2006). Early patterns of electrical activity in the developing cerebral cortex of humans and rodents. Trends Neurosci. *29*, 414–418.
20. Petersson, P., Waldenström, A., Fåhraeus, C., and Schouenborg, J. (2003). Spontaneous muscle twitches during sleep guide spinal self-organization. Nature *424*, 72–75.
21. Slater, P.J.B., and Lester, N.P. (1982). Minimising errors in splitting behaviour into bouts. Behaviour *79*, 153–161.
22. Latash, M.L., Scholz, J.P., and Schöner, G. (2007). Toward a new theory of motor synergies. Mot. Contr. *11*, 276–308.
23. Caraux, G., and Pinloche, S. (2005). PermutMatrix: a graphical environment to arrange gene expression profiles in optimal linear order. Bioinformatics *21*, 1280–1281.
24. Blumberg, M.S., and Lucas, D.E. (1994). Dual mechanisms of twitching during sleep in neonatal rats. Behav. Neurosci. *108*, 1196–1202.
25. Lemon, R.N. (2008). Descending pathways in motor control. Annu. Rev. Neurosci. *31*, 195–218.
26. Gassel, M.M., Marchiafava, P.L., and Pompeiano, O. (1965). Activity of the red nucleus during deep desynchronized sleep in unrestrained cats. Arch. Ital. Biol. *103*, 369–396.
27. Baldissera, F., Broggi, G., and Mancia, M. (1966). Monosynaptic and polysynaptic spinal reflexes during physiological sleep and wakefulness. Arch. Ital. Biol. *104*, 112–133.
28. Kubota, K., and Tanaka, R. (1968). Fusimotor unit activities and natural sleep in the cat. Jpn. J. Physiol. *18*, 43–58.
29. Gassel, M.M., Marchiafava, P.L., and Pompeiano, O. (1964). Tonic and phasic inhibition of spinal reflexes during deep, desynchronized sleep in unrestrained cats. Arch. Ital. Biol. *102*, 471–479.
30. Kiehn, O. (2011). Development and functional organization of spinal locomotor circuits. Curr. Opin. Neurobiol. *21*, 100–109.
31. Quinlan, K.A., and Kiehn, O. (2007). Segmental, synaptic actions of commissural interneurons in the mouse spinal cord. J. Neurosci. *27*, 6521–6530.
32. Bernstein, N.A. (1967). The Coordination and Regulation Of Movements (Oxford: Pergamon Press).
33. Sporns, O., and Edelman, G.M. (1993). Solving Bernstein's problem: a proposal for the development of coordinated movement by selection. Child Dev. *64*, 960–981.
34. Gibson, E.J. (1988). Exploratory behavior in the development of perceiving, acting, and the acquiring of knowledge. Annu. Rev. Psychol. *39*, 1–41.
35. Berthier, N.E., Rosenstein, M.T., and Barto, A.G. (2005). Approximate optimal control as a model for motor learning. Psychol. Rev. *112*, 329–346.
36. Schlesinger, M. (2004). Evolving agents as a metaphor for the developing child. Dev. Sci. *7*, 158–164.
37. Adolph, K., and Berger, S. (2006). Motor development. In Handbook of Child Psychology, Volume 2: Cognition, Perception, and Language, W. Damon, R.M. Lerner, D. Kuhn, and R.S. Siegler, eds. (New York: Wiley), pp. 161–213.
38. Dominici, N., Ivanenko, Y.P., Cappellini, G., d'Avella, A., Mondì, V., Cicchese, M., Fabiano, A., Silei, T., Di Paolo, A., Giannini, C., et al. (2011). Locomotor primitives in newborn babies and their development. Science *334*, 997–999.
39. MacNeilage, P.F., and Davis, B.L. (2000). On the origin of internal structure of word forms. Science *288*, 527–531.
40. Marques, H.G., Imtiaz, F., Iida, F., and Pfeifer, R. (2013). Self-organization of reflexive behavior from spontaneous motor activity. Biol. Cybern. *107*, 25–37.
41. Kuperstein, M. (1988). Neural model of adaptive hand-eye coordination for single postures. Science *239*, 1308–1311.
42. Lungarella, M., Metta, G., Pfeifer, R., and Sandini, G. (2003). Developmental robotics: a survey. Connect. Sci. *15*, 151–190.
43. Werker, J.F., and Tees, R.C. (1984). Cross-language speech perception: Evidence for perceptual reorganization during the first year of life. Infant Behav. Dev. *7*, 49–63.
44. Siegler, R.S. (1989). Mechanisms of cognitive development. Annu. Rev. Psychol. *40*, 353–379.
45. Lewkowicz, D.J., and Ghazanfar, A.A. (2009). The emergence of multisensory systems through perceptual narrowing. Trends Cogn. Sci. *13*, 470–478.
46. McMurray, B., Horst, J.S., and Samuelson, L.K. (2012). Word learning emerges from the interaction of online referent selection and slow associative learning. Psychol. Rev. *119*, 831–877.
47. Shriner, A.M., Drever, F.R., and Metz, G.A. (2009). The development of skilled walking in the rat. Behav. Brain Res. *205*, 426–435.
48. Oudiette, D., Leu-Semenescu, S., Roze, E., Vidailhet, M., De Cock, V.C., Golmard, J.-L., and Arnulf, I. (2012). A motor signature of REM sleep behavior disorder. Mov. Disord. *27*, 428–431.

Current Biology, Volume *23*

Supplemental Information

Spatiotemporal Structure of REM Sleep Twitching Reveals Developmental Origins of Motor Synergies

Mark S. Blumberg, Cassandra M. Coleman, Ashlynn I. Gerth, and Bob McMurray

Supplemental Inventory

1. Supplemental Figures

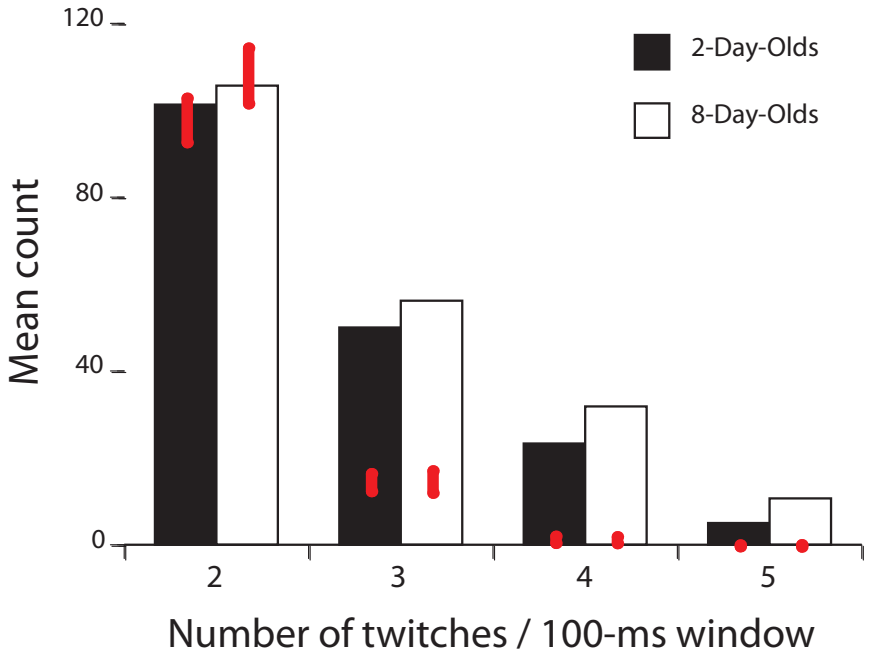

Figure S1. Quantity of multi-joint twitching in relation to chance. Presented are the mean observed counts of 100-ms windows (per pup/litter) containing 2, 3, 4, or 5 twitches in 2- (black bars) and 8-day-old (white bars) rats. Vertical red bars represent the 95% confidence intervals computed using Monte Carlo randomizations (500 iterations). In this Monte Carlo analysis, for each original twitch in the raw dataset we replaced the time with a new time drawn from a uniform distribution (range: 1-20,000 ms), and randomly selected the type of twitch (e.g., right shoulder adduction) with a 1/8 probability. At both ages, 3-, 4-, and 5-twitch events were more likely than expected by chance (*ps* < .002), whereas 2-twitch events were not (2-day-olds: $p = .14$; 8-day-olds: $p = .764$). Events containing 0-1 twitches were excluded from this analysis.

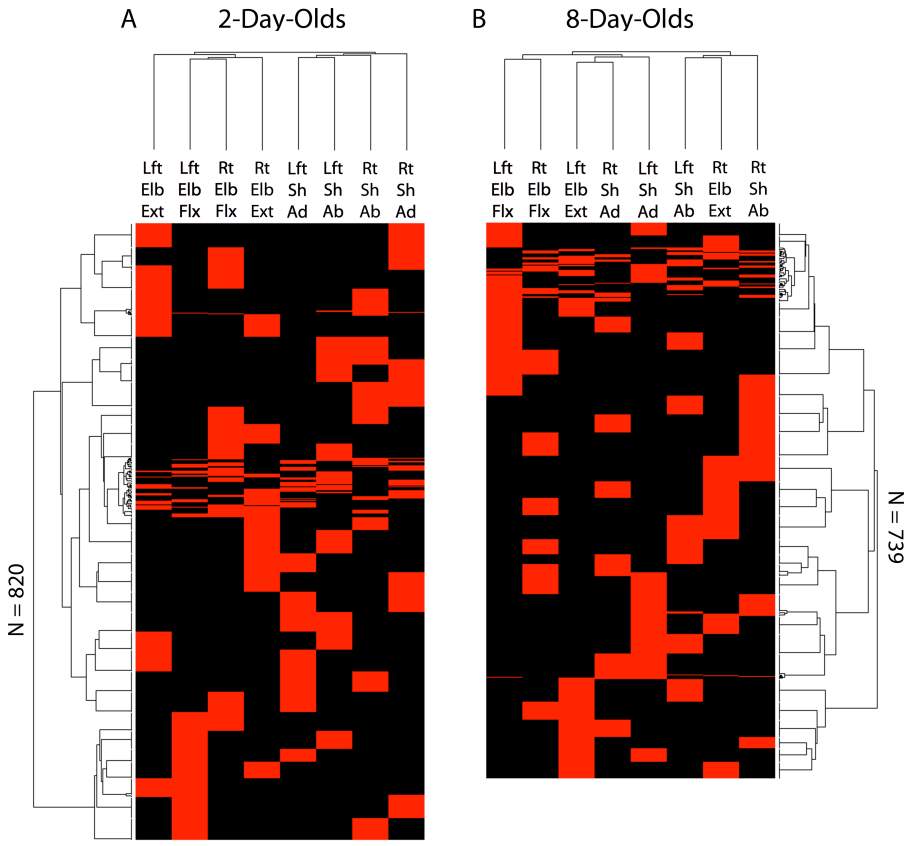

Figure S2. Randomized hierarchical cluster analyses, with seriation, of multi-joint twitching at the shoulders and elbows in (A) 2- and (B) 8-day-old rats. Data were obtained from a single run of the randomization described in Figure S1. Otherwise, these analyses were performed identically to those in Figure 5. The dendrograms at both ages are relatively unstructured (in relation to Figure 5). This is indicated in three ways. First, the large distance of leaves (i.e., individual joints) from the clades (i.e., groupings) in the top dendrograms suggests weak grouping between leaves. Second, the short distance separating clades in the top dendrograms suggests that individual clusters are not highly distinct. Finally, most clades in both the top and rotated dendrograms are simplicifolious (i.e., they comprise a single leaf added to a group, rather than two leaves combining to form a group), suggesting little similarity among individual leaves (i.e., joints in the top dendrograms or events in the rotated dendrograms). Note that there are fewer events (i.e., rows) in these plots than in Figure 5 because, after randomization, there were fewer events comprising more than one twitch and, in particular, there were far fewer events with three or more twitches; see Figure S1). Abbreviations: Rt, right; Lft, left; Sh, shoulder; Elb, elbow; Ad, adduction; Ab, abduction; Flx, flexion; Ext, extension.

2. Supplemental Tables

Table S1. The total number of 2- and 8-day-old subjects used in this study and the number of videos, twitches, and twitches/video obtained.

	Number of subjects/Number of litters	Total number of videos	Total number of twitches	Number of twitches/video
2-day-olds	10/7	35	4966	141.9
8-day-olds	6/6	39	5168	132.5

Table S2. Total number of twitches at each joint in the left and right forelimbs across all 2- and 8-day-old subjects. Ad = adduction; Ab = abduction; Ext = extension; Flx = flexion.

	Left Shoulder		Left Elbow		Left Wrist		Right Shoulder		Right Elbow		Right Wrist	
	Ad	Ab	Ext	Flx	Ext	Flx	Ad	Ab	Ext	Flx	Ext	Flx
2-day-olds	551	363	404	437	461	246	494	359	399	543	481	228
8-day-olds	509	386	473	375	429	316	514	368	458	475	515	350

3. Supplemental Movie

Movie S1. Examples of twitching in an 8-day-old rat. Five clips are shown: (i) 18 seconds of real-time twitching; (ii) a discrete twitch, in slow motion, comprising extension of the left elbow; (iii) a discrete twitch, in slow motion, comprising abduction of the right shoulder; (iv) an example, in slow motion, of a homologous twitch pattern comprising right shoulder adduction followed quickly by left shoulder adduction; and (v) an example, in slow motion, of a complex multi-joint twitch pattern comprising several movements across both forelimbs. The white dots are fluorescent paint for motion tracking of joint movements. All videos were recorded at 250 frames per second.

4. Supplemental Experimental Procedures

Experiments were carried out in accordance with the National Institutes of Health Guide for the Care and Use of Laboratory Animals (NIH Publication No. 80-23) and were approved by the Institutional Animal Care and Use Committee of the University of Iowa.

Subjects

Subjects were male and female Sprague-Dawley Norway rats (*Rattus norvegicus)*. A total of 10 P2 rats from seven litters (body weight: 6.1-8.2 g) and six P8 rats from six litters (body weight: 17.2-20.1 g) were used. Litters were culled to eight pups within three days of birth (day of birth = P0). Mothers and their litters were housed and raised in laboratory cages (36 x 27 x 21 cm; Thoren Caging Systems, Hazleton, PA) in the animal colony at the University of Iowa. Food and water were available ad libitum. All animals were maintained on a 12-h light-dark schedule with lights on at 0700 h.

Preparation of subjects for videorecording

On the day of testing and during the lights-on period, a pup with a visible milk band was anesthetized with isoflurane and secured in a supine position in a custom-made silicone mold sized appropriately to the age of the pup. Light restraints were placed over the neck and abdomen to keep the pup in place. An ultraviolet (UV) fluorescent paint was applied at key locations along the two forelimbs and chest (see Figure 1A). After this procedure, which lasted less than 10 min, the pup was transferred to a humidified incubator maintained at thermoneutrality (P2: 35.5˚C; P8: 32˚C) for testing.

Data acquisition

Two high-speed (250 frames/s) digital video cameras (Integrated Design Tools, Tallahassee, FL) with 105 mm micro-Nikkor lenses (Nikon, Melville, NY) were used. These cameras record directly to digital at 1280 x 1024 pixels. Motion Studio software (Integrated Design Tools) was used to synchronize the cameras and record videos.

Recordings began when the pup was cycling between sleep and wakefulness; cycling between states is more rapid at P2 than at P8, but at both ages sleep is the predominant state [1]. Under ultraviolet illumination, multiple 20-s recordings were acquired; this was the maximum duration allowable given camera memory (8 GB) and frame rate. During each 20-s recording period, the experimenter closely monitored the subject and confirmed that only twitches were expressed (if wake behaviors or startles were detected, the video data were not saved). When data were saved, approximately 35 minutes were needed to download the data from the two cameras, after which the next recording began. At the completion of the recording session, each pup was returned to its home cage and the cameras were calibrated for 3-D motion tracking using a calibration fixture and ProAnalyst software (Xcitex, Boston, MA).

For each of the six P8 subjects, 6-8 videos/pup were acquired. For the P2 subjects, however, the range was 2-6 videos/pup; because, in three instances at this age, subjects yielded only two videos (due to fussiness), a littermate was used to provide 2-3 additional videos, thus yielding 4-6 videos from each litter at this age. Thus, the “true” sample size—based on the number of litters rather than the number of pups used—was seven at P2 and six at P8. Although we refer to “pup” in the text (for ease of presentation), in some cases we are referring to a litter.

Data reduction

The protocol for data analysis began with automatic motion tracking of the joints using ProAnalyst 3-D software. Automatic tracking was always supplemented by frame-by-frame confirmation and, when necessary, manual correction. The calibration fixture's coordinates allowed us to pinpoint the location of each fluorescent dot on the subject's body in 3-dimensional space with an accuracy of approximately 0.1 mm.

Based on preliminary analyses, we identified six joint angles or line distances that reliably identified shoulder abduction and adduction, elbow extension and flexion, and wrist extension and flexion, for each of the two forelimbs. These angles and distances were computed using the ProAnalyst software for each of the 5000 video frames from each camera for a given 20-s recording period. Next, the data were imported into Spike2 (Cambridge Electronic Design, Cambridge, UK) as six continuous waveforms representing the six joints across the two forelimbs. To convert these continuous waveforms to discrete twitch-events that indicate movement onset times, we first filtered slow oscillations from the waveforms (time constant = 0.4 s). Next, we calculated the mean baseline quiescent activity for each waveform from multiple time-points across the 20-s recording. The threshold for estimating the onset time for each twitch-event was the standard deviation of this mean multiplied by 15. For quality control, we regularly cross-checked these onset times against video records.

Two highly trained individuals separately converted the data from waveforms to twitch-events. On a regular basis, three videos from each age group were randomly selected and, for each video, both individuals scored the same joint. Inter-rater reliability

for converting waveforms to onset times was high, with Cohen's Kappa ranging from .83 to .94 (computed using GSEQ software [2]).

Data analysis

Because of the short duration of each individual 20-s recording, most analyses were performed on pooled data at each age. Within Spike2, the pooled data at each age comprised a single datafile denoting records of onset times for each joint movement; breaks between 20-s recordings were marked to prevent inappropriate analyses across sessions. To compute inter-twitch intervals for frequency distributions, twitch onset times were interleaved to produce a single record of all twitches in both forelimbs.

For all inferential statistics, alpha was set at 0.05. All means are presented with their standard error.

Perievent histograms were used to assess pairwise relationships between joint movements. They were computed using the "event correlation" function in Spike2 with one joint movement designated the "target" and the other the "trigger." Histograms were computed using pooled data at each age, and indicate the total number of target events for each 25 ms time bin surrounding the trigger; counts were normalized to percentages in relation to the total number of target twitches within the 500-ms histogram window (250 ms before and after the trigger). To determine statistical significance, we jittered the trigger event data 1000 times within a 250-ms window using PatternJitter [3, 4] and for each jitter constructed 1000 perievent histograms (using a custom-written Matlab program). From this we established a 99% ($p < .01$) criterion, to which we compared each 50-ms bin of the actual data.

To create a windowed dataset, we stepped through the raw data in 75-ms increments. At each time point, all twitches occurring within a 100-ms window were identified (the resulting 25-ms overlap of windows functionally smoothed the data). We chose a 100-ms window based on the inter-twitch interval data (Figure 1C) and the perievent histograms showing that most pairwise twitches occurred within this window (Figures 2 and 3); however, we also examined shorter and longer windows to confirm that our findings were not overly sensitive to this choice. Before analysis, we eliminated windows containing either no twitches or a single twitch. Eliminating these windows amplified the probabilities of multi-twitch events (our primary interest) without changing the relative likelihoods of different types of multi-twitch events. The resulting dataset represented 49.5% of the full set of windows at P2 and 46.4% at P8. The final windowed datasets were composed of 1269 rows at P2 (mean = 181.3 $\pm$ 22.2 rows/pup) and 1242 rows at P8 (mean = 207.0 $\pm$ 21.7 rows/pup). These rows are referred to as "events" below and in the main text.

To examine age-related changes in twitching, we calculated the mean proportion of 100-ms events (in the windowed dataset) that, for example, contained shoulder abductions in the left and right forelimb. These were calculated using the pup/litter as the unit of analysis. Proportions were transformed using the empirical logit and ANOVAs and t tests were performed were performed using SPSS (IBM, Endicott, NY).

Although we examined many different movement categories, only a subset comprising the most clear and significant results are described in the main text.

Hierarchical cluster analysis (HCA) with seriation was performed using PermutMatrix software [5]. The settings used were Euclidean distance and Ward's

Minimum Variance Method. For seriation, the multiple-fragment heuristic was used. Each row of the data was treated as an independent observation for this analysis.

Latent class analysis (LCA) was performed using Latent GOLD software (Statistical Innovations, Belmont, MA). The data at P2 and P8 were analyzed separately and litter was used as the random effect. Cluster convergence occurred for both datasets and the determination of the best model fit was made based by minimizing the value of the Akaike Information Criterion (AIC). We also confirmed that none of the bivariate residuals exceeded a value of 1, indicating that all eight joint movements were independent of each other. The best model fits yielded 28 clusters at P2 and 21 clusters at P8. Each cluster was visualized as a profile plot.

To test whether the clusters produced by LCA were simply due to the relative independent frequencies of the twitch movements, we used a Monte Carlo method to determine the likelihood of a particular cluster appearing by chance. To do this, we shuffled the assignment of twitches to event times within each 20-s video segment. This conservative approach maintained the relative frequencies of the different twitches (e.g., in the shuffled dataset elbow flexion occurred just as frequently, but at different times) and the temporal structure of the datasets (e.g., if twitches tended to come in sets of three within a 100-ms window, that continued to be the case), but the particular limbs involved were now variable. Shuffling was performed 150 times and LCA was performed on each of the shuffled datasets. Then, for each LCA twitch pattern (or cluster) identified from the original dataset, we determined whether that pattern could have arisen by chance by assessing its likelihood against all of the twitch patterns that LCA detected in the 150 shuffled datasets. (Clusters were matched between the original

dataset and the clusters from the LCA analyses of each of the 150 Monte Carlo runs by converting each cluster, in either set, to a discrete series of joints based on an upper and lower threshold. A range of thresholds was used to ensure that our results were robust.) Even using this conservative method, nearly all of the clusters that LCA identified were unlikely to have arisen by chance ($p < .05$). We conclude that LCA properly identified clusters.

In order to examine developmental changes in the clusters of twitches, we needed to match P2 and P8 clusters. Thus, we tested the similarity of each of the 28 clusters at P2 against each of the 21 clusters at P8, and vice versa, using the eight probability values that comprise each profile plot as the basis of similarity. Two similarity rules were used. First, we used Euclidean distance. Second, since Euclidean distance assumes a linear scaling that may not be appropriate for probabilities, we also used a probabilistic rule (Equation 1) in which similarity was the probability of the same twitch being present (in each cluster) added to the probability that the same twitch was absent from both:

$$Similarity_{x \leftrightarrow y} = \sum_{t \in twtiches} p^t{}_x p^t{}_y + \left(1 - p^t{}_x\right)\left(1 - p^t{}_y\right) \quad (1)$$

Here, $p^t{}_x$ represents the probability that twitch t (e.g., elbow flexion) participated in cluster x (one of the clusters from the P2 analysis) or cluster y ($p^t{}_y$, from the P8 analysis). Combined, this computes the probability that both twitches occurred ($p^t{}_x p^t{}_y$) or that neither did ($[1-p^t{}_x][1-p^t{}_y]$), summed over all eight pairs of corresponding twitches within a given pair of clusters.

A P2 and P8 cluster were deemed a match only if they were the best matches on both similarity rules exclusively and reciprocally (i.e., the P2 cluster's closest match was

the P8 cluster, and the P8 cluster's closest match was the P2 cluster).

Regression analyses of the LCA clusters were performed using SPSS. We computed Shannon's Entropy, *E,* for each cluster by first normalizing the probabilities associated with each twitch (for a given cluster) by dividing each probability by the sum of the probabilities. (Note that in these profile probabilities, each likelihood represents the independent probability of a specific joint movement given the cluster. The LCA coefficients for a given cluster represent eight binomial distributions, not a single multinomial distribution.) We next calculated *E* using Equation 2:

$$E_x = -\sum_n q^n{}_x \log_2\left(q^n{}_x\right) \quad (2)$$

Here, E_x is the entropy of cluster *x*; and $q^n{}_x$ is the normalized probability of twitch *n*, in cluster *x,* output from the LCA (after normalization).

Cluster frequency was obtained from Latent Gold LCA software and was log-transformed prior to analysis.

5. Supplemental References

1. Blumberg, M. S., Seelke, A. M. H., Lowen, S. B., and Karlsson, K. Æ. (2005). Dynamics of sleep-wake cyclicity in developing rats. Proc. Natl. Acad. Sci. USA *102*, 14860–14864.

2. Bakeman, R., and Quera, V. (2011). *Sequential analysis and observational methods for the behavioral sciences* (Cambridge: Cambridge University Press).

3. Harrison, M. T., and Geman, S. (2009). A rate and history-preserving resampling algorithm for neural spike trains. Neural Comput. *21*, 1244–1258.

4. Amarasingham, A., Harrison, M. T., Hatsopoulos, N. G., and Geman, S. (2012). Conditional modeling and the jitter method of spike resampling. J. Neurophysiol. *107*, 517–531.

5. Caraux, G., and Pinloche, S. (2005). PermutMatrix: a graphical environment to arrange gene expression profiles in optimal linear order. Bioinformatics *21*, 1280–1281.